Received: 13 July 2022 | Accepted: 14 December 2022

DOI: 10.1111/ede.12427

RESEARCH ARTICLE

WILEY

Teeth outside the mouth: The evolution and development of shark denticles

Rory L. Cooper[1] | **Ella F. Nicklin**[2] | **Liam J. Rasch**[3] | **Gareth J. Fraser**[2]

[1]Department of Genetics and Evolution, The University of Geneva, Geneva, Switzerland

[2]Department of Biology, University of Florida, Gainesville, Florida, USA

[3]Division of Cardiovascular Medicine, University of Virginia, Charlottesville, Virginia, USA

Correspondence
Gareth J. Fraser, Department of Biology, University of Florida, Gainesville, FL, USA.
Email: g.fraser@ufl.edu

Funding information
Leverhulme Trust, Grant/Award Number: RPG-211; National Science Foundation, Grant/Award Number: 2128032; Natural Environment Research Council, Grant/Award Number: NE/K014595/1

Abstract

Vertebrate skin appendages are incredibly diverse. This diversity, which includes structures such as scales, feathers, and hair, likely evolved from a shared anatomical placode, suggesting broad conservation of the early development of these organs. Some of the earliest known skin appendages are dentine and enamel-rich tooth-like structures, collectively known as odontodes. These appendages evolved over 450 million years ago. Elasmobranchs (sharks, skates, and rays) have retained these ancient skin appendages in the form of both dermal denticles (scales) and oral teeth. Despite our knowledge of denticle function in adult sharks, our understanding of their development and morphogenesis is less advanced. Even though denticles in sharks appear structurally similar to oral teeth, there has been limited data directly comparing the molecular development of these distinct elements. Here, we chart the development of denticles in the embryonic small-spotted catshark (*Scyliorhinus canicula*) and characterize the expression of conserved genes known to mediate dental development. We find that shark denticle development shares a vast gene expression signature with developing teeth. However, denticles have restricted regenerative potential, as they lack a *sox2*+ stem cell niche associated with the maintenance of a dental lamina, an essential requirement for continuous tooth replacement. We compare developing denticles to other skin appendages, including both sensory skin appendages and avian feathers. This reveals that denticles are not only tooth-like in structure, but that they also share an ancient developmental gene set that is likely common to all epidermal appendages.

KEYWORDS
dermal denticles, skin appendages, tooth development

1 | INTRODUCTION

Vertebrate skin appendages are an incredibly diverse group of organs that adorn the integument, including scales, spines, hair, feathers, and teeth. Despite dramatic variety in both their form and function, the early development of vertebrate skin appendages is widely characterized by the emergence of an anatomical placode (Cooper et al., 2017; Di-Poï & Milinkovitch, 2016; Harris et al., 2008); a local epidermal thickening associated with conserved gene expression patterns in both the epidermis and underlying dermis. This placode constitutes the

common foundation of phylogenetically distinct skin appendages (Cooper et al., 2017). Furthermore, reaction-diffusion-like dynamics are broadly considered to control the spatial distribution of placode emergence (Cooper et al., 2018; Kondo, 2002; Sick et al., 2006).

Odontodes can be defined as "special hard tissue units, or dental units, which generally speaking have those developmental and structural properties in common with the teeth of the jaws" (Ørvig, 1977). These structures constitute one of the earliest known vertebrate skin appendage types (Sansom et al., 1996). Odontodes are hard, mineralized, tooth-like structures evolved in extinct early jawless fishes from which jawed vertebrates later evolved. In extant jawed-vertebrates, they include both oral teeth, branchial/pharyngeal denticles (Fraser et al., 2010), and modified enamel/dentine derived scales in certain clades of bony fishes (Chen et al., 2020; Mori & Nakamura, 2022). Furthermore, odontodes include hard, mineralized scales (or "skin-teeth") that adorn the bodies of elasmobranchs (sharks, skates, and rays), known as dermal denticles. These denticles consist of a hard outer layer of hyper-mineralized enamel-like tissue (Gillis & Donoghue, 2007), a dentine layer, and a central pulp cavity, making them structurally homologous to vertebrate teeth (Fraser et al., 2010). The denticles of adult sharks facilitate numerous functions, including hydrodynamic drag reduction during locomotion, the provision of defensive armor, and communication via the binding of luminescent photophores (Oeffner & Lauder, 2012; Reif, 1985; Wen et al., 2015). Consequently, the dermal denticles of elasmobranchs have evolved to exhibit various shapes and sizes, both within and across species (Gabler-Smith et al., 2021; Motta et al., 2012). Patterns of morphological variation in shark denticles are also observable across deep time (Sibert & Rubin, 2021). Although the early development and patterning of shark denticles has been previously characterized (Cooper et al., 2017, 2018), the molecular basis of their development, morphogenesis, and final morphological diversity is not yet comprehensively understood.

The elasmobranch dentition is renowned for its prolific conveyor belt-like system of continuous tooth replacement, regulated by the maintenance of a stem cell population in the dental lamina, an essential structure for dental regeneration (Fraser et al., 2020; Rasch et al., 2016). This stem cell population is characterized by the expression of sex-determining region Y-related box 2 (*sox2*), an epithelial progenitor and stem cell marker (Juuri et al., 2013; Martin et al., 2016). Conversely, dermal denticles do not arise from a dental lamina and do not exhibit a continuous replacement mechanism. Instead, new denticles are thought to arise either as a result of growth of the body, denticle loss, or after wounding (Reif, 1978). Although a common odontode gene regulatory network (oGRN) (Fraser et al., 2010) appears to underpin the conserved development of both teeth and denticles, only teeth retain the ancestral gnathostome character of continuous successional tooth regeneration (Martin et al., 2016).

Contrasting theories have been presented regarding the evolutionary origins of odontodes (Donoghue & Rücklin, 2016). One such theory suggests that external dermal odontodes arose first, before odontode-competent ectoderm subsequently migrated inside the oral cavity to form teeth (the "outside-in" hypothesis). Conversely, it has previously been suggested that odontodes first arose inside the pharyngeal cavity in extinct jawless fishes, separately from dermal denticles (the "inside-out" hypothesis) (Donoghue & Rücklin, 2016; Fraser et al., 2010; Smith & Coates, 1998, 2000, 2001). This uncertainty arose due to contrasting fossil evidence from early jawless vertebrates (Donoghue, 2002; Donoghue & Rücklin, 2016; Sire et al., 2009; Smith & Coates, 1998). However, the inside-out hypothesis incorrectly assumed that conodonts possessed tooth homologs, meaning the inside-out hypothesis has since been rejected (Donoghue & Rücklin, 2016; Murdock et al., 2013). It is now understood that odontodes can develop both inside and outside of the oral cavity (the "inside and out" hypothesis), wherever conserved and co-expressed members of the underlying oGRN are present (Donoghue & Rücklin, 2016; Fraser et al., 2010). Importantly, studies examining the development of odontodes at the molecular and cellular levels have significant implications regarding the evolutionary origins of these skin appendages (Martin et al., 2016; Rasch et al., 2016).

Despite the structural similarities that exist between elasmobranch dermal denticles and oral teeth, there remains limited data directly comparing the embryonic development of these distinct structures, although previous work has demonstrated various gene expression patterns associated with their initiation and morphogenesis (Debiais-Thibaud et al., 2011, 2015; Martin et al., 2016). Here, we use immunohistochemistry (IHC) and in situ hybridization (ISH) to characterize the cellular and molecular processes that underpin denticle development in the embryonic small-spotted catshark (*Scyliorhinus canicula*). The gene pathways examined here have been selected based on mammalian studies of dental development (Yu & Klein, 2020), although conservation of core molecular signaling during elasmobranch tooth development has now been described (Rasch et al., 2016, 2020; Thiery et al., 2022). Despite superficial differences in their form and function, we suggest that the early development and morphogenesis of shark odontodes is underpinned by the conserved expression patterns of a

shared suite of developmental genes that comprise an oGRN, linking the molecular development of both teeth and scales.

2 | METHODS

2.1 | Shark and chicken husbandry

The University of Sheffield is a licensed establishment under the Animals (Scientific Procedures) Act 1986. All animals were culled by approved methods cited under Schedule 1 to the Act. *S. canicula* embryos were purchased from North Wales Biologicals, UK, and raised in oxygenated artificial saltwater (Instant Ocean) at 16°C. Embryos were culled using MS-222 (Tricaine) at 300 mg/l and fixed overnight in 4% paraformaldehyde in phosphate-buffered saline (PBS). Fertilized Bovan brown chicken eggs were purchased from Henry Stewart & Co., incubated at 37.5°C, and fixed overnight in Carnoy's solution. Following fixation, shark and chicken embryos were dehydrated through a graded series of PBS to ethanol (EtOH) and stored at −20°C.

2.2 | Scanning electron microscopy (SEM)

SEM was undertaken using a Hitachi TM3030Plus Benchtop SEM scanner at 15,000 V. Global brightness and contrast adjustments, and the addition of scalebars, was undertaken using Fiji (Schindelin et al., 2012).

2.3 | Alizarin red clear and staining

Fixed, dehydrated shark embryos were rehydrated into PBS and stained overnight in alizarin red in potassium hydroxide (KOH), as previously described (Cooper et al., 2017). Imaging was conducted using a Nikon SMZ15000 stereomicroscope, and scale bars were created using Fiji (Schindelin et al., 2012).

2.4 | Microcomputed tomography (Micro-CT)

Micro-CT scanning was undertaken using shark samples stained with 0.1% phosphotungstic acid (PTA) as previously described (Cooper et al., 2017), using an Xradia MicroXCT scanner at the Imaging and Analysis Center of the Natural History Museum. Rendering was undertaken using the 3D volume exploration tool Drishti (www.github.com/nci/drishti).

2.5 | Immunohistochemistry (IHC)

IHC of paraffin sections was undertaken as previously described (Rasch et al., 2016). Sections were imaged with an Olympus BX51 Upright Compound Microscope and Olympus DP71 Universal digital camera attachment. Fiji was used to globally adjust brightness and contrast and to add scale bars (Schindelin et al., 2012).

2.6 | ISH

The design of digoxigenin-labeled antisense riboprobes and subsequent whole mount ISH was undertaken as previously described (Cooper et al., 2017, 2018). Riboprobes were designed using partial skate (*Leucoraja erinacea*) and catshark (*S. canicula* or *Scyliorhinus torazame*) EST assemblies (Wyffels et al., 2014) (SkateBase, skatebase.org), and the Vertebrate TimeCapsule (VTcap, transcriptome.cdb.riken.go.jp/vtcap). The riboprobes were cloned from *S. canicula* cDNA using the primer sequences shown in Table 1. Sections were imaged with an Olympus BX51 Upright Compound Microscope and Olympus DP71 Universal digital camera attachment. Whole mount samples were imaged using a Nikon SMZ15000 stereomicroscope. Fiji was used to globally adjust brightness and contrast and to add scale bars (Schindelin et al., 2012). Riboprobes were cloned from *S. canicula* cDNA and submitted to GenBank (NCBI) with the following accession numbers: OP716943-OP716953 and OP727297 (*fgf4*; Cooper et al., 2018). *shh* riboprobe was cloned based on the GenBank submission accession number HM991336.1 (Gillis et al., 2011).

2.7 | Whole mount ISH

The design of digoxigenin-labeled antisense riboprobes and subsequent whole mount ISH was undertaken as previously described (Cooper et al., 2017, 2018). Unless stated otherwise, denticle tissue originates from the dorsal region of the embryonic sharks, close to the dorsolateral denticle rows. Please refer to Ballard's *S. canicula* normal series of development for further information regarding total sample length at different developmental stages (Ballard et al., 1993). Samples were imaged using a Nikon SMZ15000 stereomicroscope. Fiji was used to

TABLE 1 Primer sequences and GenBank Accession numbers for *Scyliorhinus canicula* riboprobes.

Probe	Forward	Reverse	GenBank accession
βcat	GGACAAGGGTTCCTAGAAGA	GGTGAAAATGCTTGGGTCT	OP716947
bmp4	GATCAGCAGGCTCCTCGAC	TCGAGTTCAGGTGGTC	OP716943
fgf3	CTTGCTCAACAGTCTTAAGTTA	CGGAGGAGGCTCTACTGT	OP716951
lef1	GGGCTTTCTGCTGACTGATG	CGTAAGGAGCGGCAACTTC	OP716944
mk	GACAGGGTCCTCTGAAGCTG	TTAGGGTTCCATTGCGAGTC	OP716946
ptch2	TGTTGGTGGCATTATCAGTAG	GAGAAGGATGGAAGTTATGGTTAT	OP716948
shh	GTGGCAGATACGAAGGGAAG	AGGTGCCGGGAGTACCAG	HM991336.1
sox2	GAGCCGTTCATGTAGGTCTGAG	GCGCTGGAGTCAACCAGAG	OP716950
foxq1	TTTCCAATCGCTCAACGAG	GCGATTTCGATCTTGTAGGG	OP716952
runx2	GCTTTACTCCTCCGTCCA	GGCTTCTGTCTGTGTCTTC	OP716953
sostdc1	GGAGCAGGAGGAACACACC	TTTGCCTCTGGATCTTCTCTTG	OP716945
twist	TGCAGGAAGATTCCAATTCC	CGGTTCACAACATTCAGAGC	OP716949
fgf4	ATGTTGATCAGGAAGCTGCG	GTATGCGTTGGATTCGTAGGC	OP727297

globally adjust brightness and contrast and to add scale bars (Schindelin et al., 2012).

2.8 | Whole mount immunofluorescence

Samples were rehydrated from EtOH through a graded series of PBS with 0.5% Triton (PBST) and treated with 10 μg/ml proteinase k for 20 min. Samples were then incubated in 5% goat serum with 1% bovine serum albumin in PBS for the blocking stage. Primary antibody staining took place for 2 days at 4°C, using both Anti-SHH (AV44235, Sigma-Aldrich) and Anti-PCNA (ab29, Abcam) at a concentration of 1:500. Incubation in the secondary antibody was performed under the same conditions, using goat anti-mouse Alexa Fluor 488 and goat anti-rabbit Alexa Fluor 647 (Thermo Fisher) respectively. Samples were counterstained with DAPI before imaging with a Zeiss LMS 880 with Airyscan. Images shown in Figure 7 were composed using the standard deviation projection of a Z-series in Fiji (Schindelin et al., 2012).

3 | RESULTS

3.1 | Odontode diversity in the small-spotted catshark

First, we use a combination of SEM and micro-CT, to explore odontode diversity in the small-spotted catshark (*S. canicula*) (Figure 1). *S. canicula* exhibits various different odontode types that can be broadly organized into four distinct categories: (a) transient denticles of the caudal tail, (b) enlarged denticles of the dorsal trunk, (c) adult-type body denticles, which exhibit multiple forms, and (d) multicuspid oral teeth (Ballard et al., 1993; Cooper et al., 2017).

Caudal denticles of the posterior tail are the first odontode type to appear, arising between 52 and 60 days post fertilization (dpf), in two dorsal and ventral rows positioned laterally on either side of the tail fin tip (Figure 1a) (Johanson et al., 2007). Caudal denticles are placode-derived skin appendages (Cooper et al., 2017) with, typically, between 9 and 13 units forming on either dorsal row, and between 5 and 10 units forming on either lateral row (Ballard et al., 1993). These flattened units develop sequentially from posterior to anterior, approximately equidistant from one another, and exhibit highly irregular, posterior facing cusps. Caudal denticles contain an ancient dentine type constructed from tubules that exhibit a distinct branching pattern associated with the earliest known sharks from the Ordovician and Silurian. Therefore, these denticles are considered an ancestral odontode type (Johanson et al., 2008). Interestingly, these are transient units that are lost close to the time of hatching, when adult-type body denticles arise to occupy their positions.

Two dorsolateral rows of enlarged denticles on the dorsal trunk are the second odontode type to appear, between 60 and 80 dpf (Figure 1b) (Ballard et al., 1993; Enault et al., 2016). These units lack distinct ridges and have a rounded posterior-facing cusp. They are

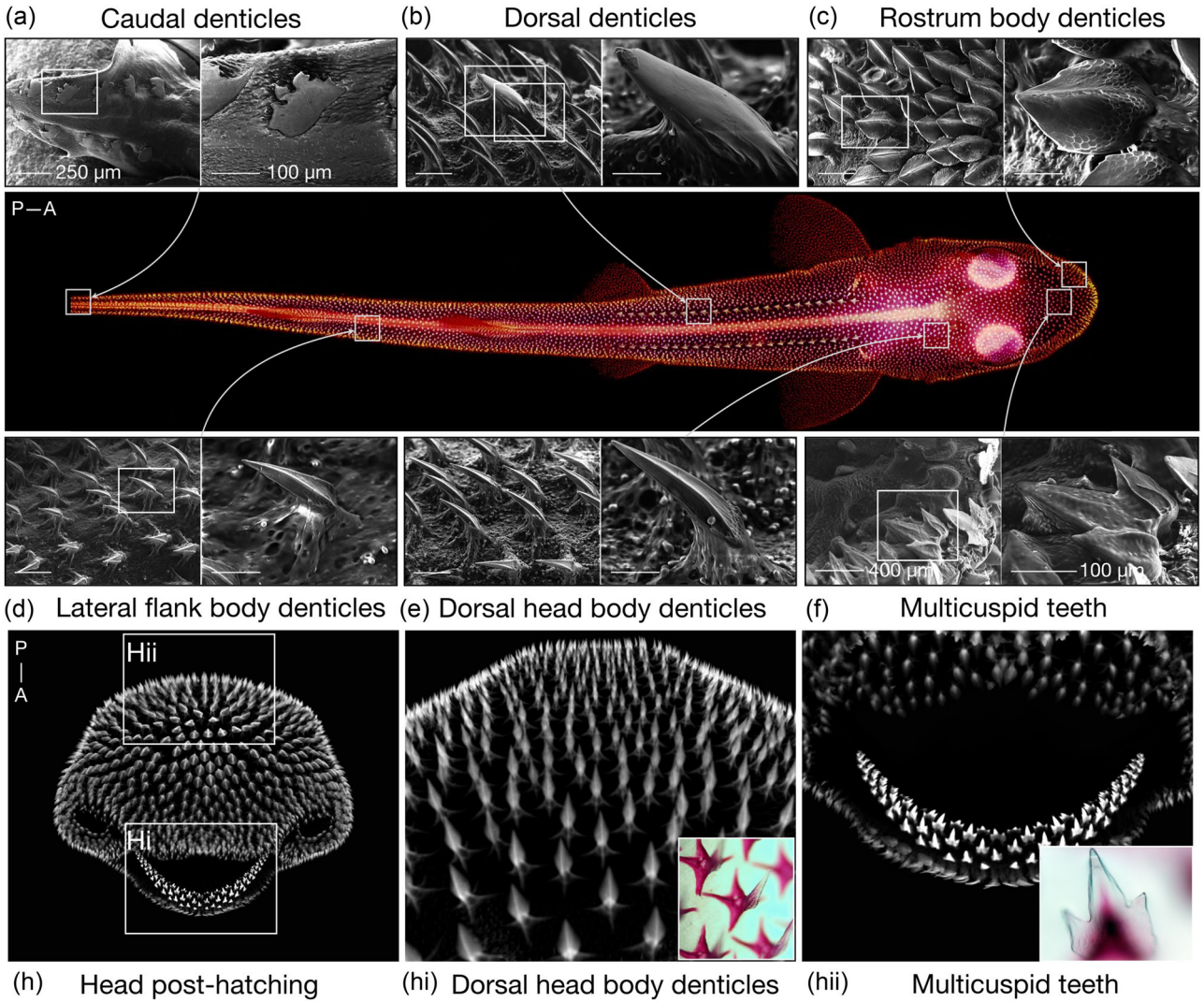

FIGURE 1 Odontode diversity of the small-spotted catshark. Scanning electron microscope (SEM) is used to reveal odontode diversity in the shark. Caudal denticles are the first odontode type to appear, in two lateral and dorsal rows, either side of the tip of the tail (a). These flattened units possess irregular posterior facing cusps, and an ancient dentine type associated with sharks from the Silurian and Ordovician (Johanson et al., 2008). Two dorsolateral rows of enlarged denticles with rounded cusps next appear on the dorsal trunk (b). These dorsal rows initiate the wider propagation of body denticles (c–e) (Cooper et al., 2018), which exhibit diverse forms while consistently displaying a single cusp. Multicuspid teeth appear close to 110 dpf, initially with a tricuspid morphology (f), although cusp number increases with tooth replacement (Thiery et al., 2022). This odontode diversity is also shown with micro-CT of the shark head (h), in which diverse body denticle types (hi) and multiple generations of multicuspid teeth (hii) are visible. All data are shown for embryonic shark specimens of ~130 dpf, except for panel (a) which shows a shark embryo of approximately ~100 dpf. Insets in panels hi and hii show alizarin red stained denticles and teeth, respectively. The P–A axis refers to sample orientation, with A being anterior and P being posterior. The whole hatchling shark is an alizarin red preparation.

subsumed into general scalation shortly after hatching (Martin et al., 2016). Dorsal denticles act as initiator rows, triggering the subsequent emergence of body denticles via a Turing-like reaction-diffusion system (Cooper et al., 2018), comparable to the patterning of avian feathers and scales (Cooper et al., 2019; Jung et al., 1998).

Body denticles are the last denticle type to arise, and are visible propagating across the entire body surface at approximately 100 dpf (Figure 1c–e,h) (Cooper et al., 2018). They exhibit dramatic variation in their morphology (Gabler-Smith et al., 2021), ranging from the petal-like denticles of the rostrum (Figure 1c) to the sharp, protruding denticles of the dorsal head surface (Figure 1d,h) and lateral flank (Figure 1e) which exhibit distinct ridges, likely associated with hydrodynamic drag reduction (Oeffner & Lauder, 2012; Wen et al., 2015). Although body denticles exhibit substantial

morphological variation, they typically display a single posterior facing cusp (Figure 1c–e,h). Conversely, oral teeth, which appear at approximately 110 dpf, are initially tricuspid (Figure 1f,hii). However, after multiple rounds of tooth replacement, five or more cusps can be observed (Thiery et al., 2022). Overall, we report a vast diversity of odontode morphologies within a single shark species.

3.2 | Cell proliferation dynamics throughout dorsal denticle development

Next, we use IHC for proliferating cell nuclear antigen (PCNA) to understand the cellular and tissue layer proliferative processes involved in dorsal denticle initiation and morphogenesis in the embryonic shark (Figure 2).

Denticle placode initiation is marked by localized epithelial and mesenchymal cell proliferation. Basal epithelial cells become columnar, producing a localized thickening of the epidermis, associated with an underlying dermal cellular condensation (Figure 2a). Early morphogenesis involves the evagination of the placode (Figure 2b), followed by onset of growth polarity and a reduction in cell proliferation in the distal epithelial tip, shown by reduced PCNA immunoreactivity (Figure 2c, red arrow). Subsequent morphogenesis is further accompanied by progressive enclosure of the proliferating mesenchymal compartment (Figure 2d). Interestingly, this non-proliferative region of the denticle cusp is indicative of a signaling center comparable to the enamel knot, a conserved mediator of tooth cusp formation (Jernvall & Thesleff, 2012; Thiery et al., 2022; Vaahtokari et al., 1996). As polarized growth continues, a reduction of PCNA immunoreactivity in the epithelial tip is maintained (Figure 2e). Throughout advancing morphogenesis, a total reduction in PCNA immunoreactivity in both the epithelium and mesenchyme implies terminal differentiation of cells to ameloblasts and odontoblasts,

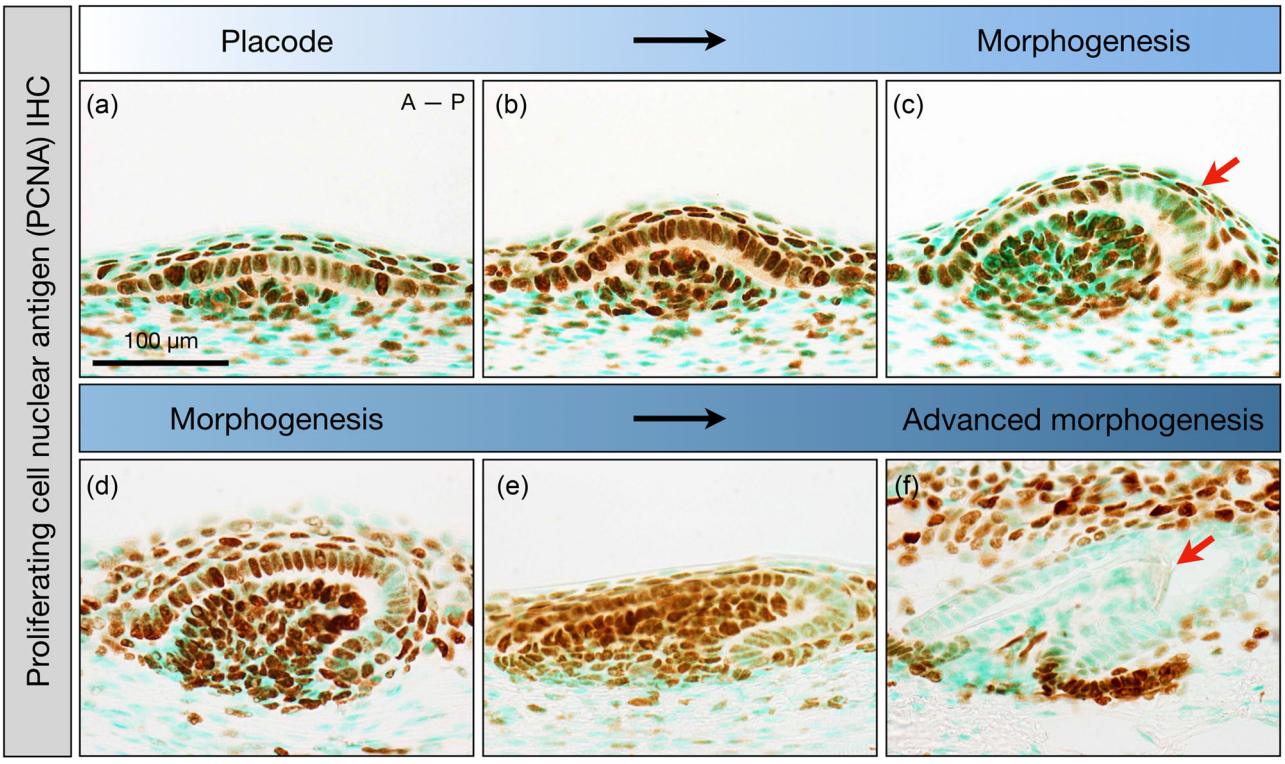

FIGURE 2 Cell proliferation during dorsal denticle development. Immunohistochemistry (IHC) for proliferating cell nuclear antigen (PCNA) is used to examine proliferative processes involved in dorsal denticle development. Denticle placode initiation is marked by a local epithelial thickening, associated with an underlying dermal condensation (a). Continued cell proliferation underpins the evagination of the epidermis and condensing dermis (b). Onset of morphogenesis is marked by asymmetric outgrowth, accompanied by reduced cell proliferation in the distal epithelial tip, in contrast to the adjoining epithelium and underlying mesenchyme (c, red arrow). This reduced proliferation continues, focal to the epithelial tip (d, e). Following advanced morphogenesis (e), cell proliferation in both the epithelium and mesenchyme is negligible, marked by a total lack of PCNA immunoreactivity of the denticle unit (f). Secreted mineralized tissue can be seen in the papilla (f, red arrow) suggesting terminal differentiation of cells to ameloblasts and odontoblasts. The A–P axis refers to sample orientation, with A being anterior and P being posterior.

respectively (Figure 2f). Corresponding matrix deposition in the papilla is also apparent (Figure 2f, red arrow). Overall, these results suggest comparable proliferative developmental processes between both dermal denticle and oral tooth cusp formation (Thiery et al., 2022).

3.3 | Conserved patterns of tooth-associated gene expression are deployed throughout denticle development

To explore the potential deployment of a shared genetic toolkit common to all odontodes, the expression patterns of genes representing several signaling pathways were investigated during body denticle development using *IS*H (Figure 3). We examined the expression of genes known to be involved in both epithelial and mesenchymal contributions to mammalian and nonmammalian tooth development (Jernvall & Thesleff, 2000). For a schematic view of general denticle structure and a summary of subsequently described gene expression patterns, please refer to Figure 4e.

Sonic hedgehog (*shh*) is a well-known facilitator of epithelial appendage patterning and development (Busby et al., 2020; Chiang et al., 1999; Chuong et al., 2000), and is specifically expressed at several key stages of tooth development (Cho et al., 2011; Smith et al., 2009; St-Jacques et al., 1998). It has also been observed in the developing caudal denticles of the catshark (Cooper et al., 2017; Johanson et al., 2008). Here, we observe *shh* in early developing body denticle placodes, and subsequently in the apical cells (central inner dental epithelial cells equivalent to the Apical Epithelial Knot [AEK] described in the shark tooth [Thiery et al., 2022]), of the early denticle bud (Figure 3ai,ii). As the bud advances through morphogenesis, *shh* expression becomes restricted to a distinct region of the epithelium, showing an initial polarity bias toward the posterior aspect of the apex (Figure 3aiii,iv). Throughout advanced morphogenesis, *shh* expression persists in the AEK, localizing to the polarized distal epithelial tip and spreading to neighboring cells at the cusp apex (Figure 3aiv–vii). Shh signals to target cells via its receptor, patched 2 (Ptch2) (Ingham & Mcmahon, 2001). Here, *ptch2* expression is present within the basal mesenchyme of the denticle papilla (Figure 3bi,ii), and is weakly expressed within cells surrounding the *shh*+ apex epithelium.

Fibroblast growth factor 3 (Fgf3) is a highly conserved member of the fibroblast growth factor family of signaling molecules, expressed during tooth cusp, hair follicle, feather bud and caudal denticle development (Bei & Maas, 1998; Cooper et al., 2017; Fraser et al., 2013; Jackman et al., 2004; Kettunen et al., 2000; Mandler & Neubüser, 2004; Rosenquist & Martin, 1996). During denticle development, *fgf3* expression is first detected at the placode stage during denticle development, localized in both the epithelium and underlying medial mesenchyme (Figure 3ci). As denticle morphogenesis progresses, *fgf3* expression spreads to encompass more of the papillary mesenchyme, accompanied by a marked increase in expression concentrated in the apex of the denticle epithelium (Figure 3cii). Throughout subsequent morphogenesis, the polarized epithelial-mesenchymal expression pattern of *fgf3* progressively increases (Figure 3ciii), before finally becoming restricted entirely to the mesenchymal papilla (Figure 3civ).

The intracellular signal transducer of the Wnt signaling pathway, β-catenin (βcat), is required for the initiation and morphogenesis of hair follicles, feather buds and teeth (Chen et al., 2012; Järvinen et al., 2006; Millar et al., 1999; Noramly et al., 1999). Developing denticles show intense *βcat* expression associated with all developmental stages, from the early placode to later stages of morphogenesis (Figure 3d). Expression is first restricted to the basal epithelium of each placode-forming unit (Figure 3di). Throughout subsequent stages of bud formation, this epithelial expression is sustained, further spreading to the underlying condensed mesenchyme and the developing papilla (Figure 3dii,iii). By advanced morphogenesis, *βcat* expression is completely absent from the epithelium, restricted instead to the basal mesenchyme of the denticle papilla (Figure 3div).

Throughout activation of Wnt signaling, nuclear *βcat* activates target genes by binding with lymphoid enhancing factor 1 (Lef1), which is also prominently expressed during both tooth and feather development (Chen et al., 2009; Handrigan & Richman, 2010; Seidensticker & Behrens, 2000). During development of denticle primordia, *lef1* is initially expressed in a similar pattern to *βcat*, marking individual placodes via expression in the basal epithelium (Figure 3ei,ii). However, throughout subsequent outgrowth *lef1* becomes restricted to the epithelial cells of the denticle placode (Figure 3eii,iii). By advanced morphogenesis, *lef1* expression is primarily restricted to two bilateral regions of the basal mesenchyme adjacent to the papilla (Figure 3eiv).

The secreted sclerostin domain-containing protein 1 (Sostcd1/Ectodin/Wise) interacts with bone morphogenic protein (BMP), Wnt, FGF, and Shh signaling to regulate the spatial patterning and morphogenesis of teeth, and the development of other epithelial appendages (Ahn et al., 2010; Cho et al., 2011; Mou et al., 2011; Munne et al., 2009). In shark denticle development, *sostdc1* is expressed in the basal epithelium of the placode (Figure 3fi). During early growth, expression shifts bilaterally to the peripheral epithelium (equivalent to

the outer dental epithelium [ODE] in teeth), leaving a central apical region devoid of expression (Figure 3fii,iii). By advanced morphogenesis, *sostdc1* becomes predominantly restricted to the posterior in-fold of the epithelium toward the base of the denticle cusp (Figure 3fiv).

The heparin-binding growth factor Midkine (Mk) regulates various aspects of cell growth and differentiation and is also expressed throughout different stages of tooth development (Mitsiadis et al., 1995, 2008; Park et al., 2020). Throughout denticle development, *mk* expression is first observed in the thickened epithelium of denticle placodes, with expression also noted in the underlying mesenchyme (Figure 4ai). Mesenchymal expression of *mk* subsequently expands to encompass

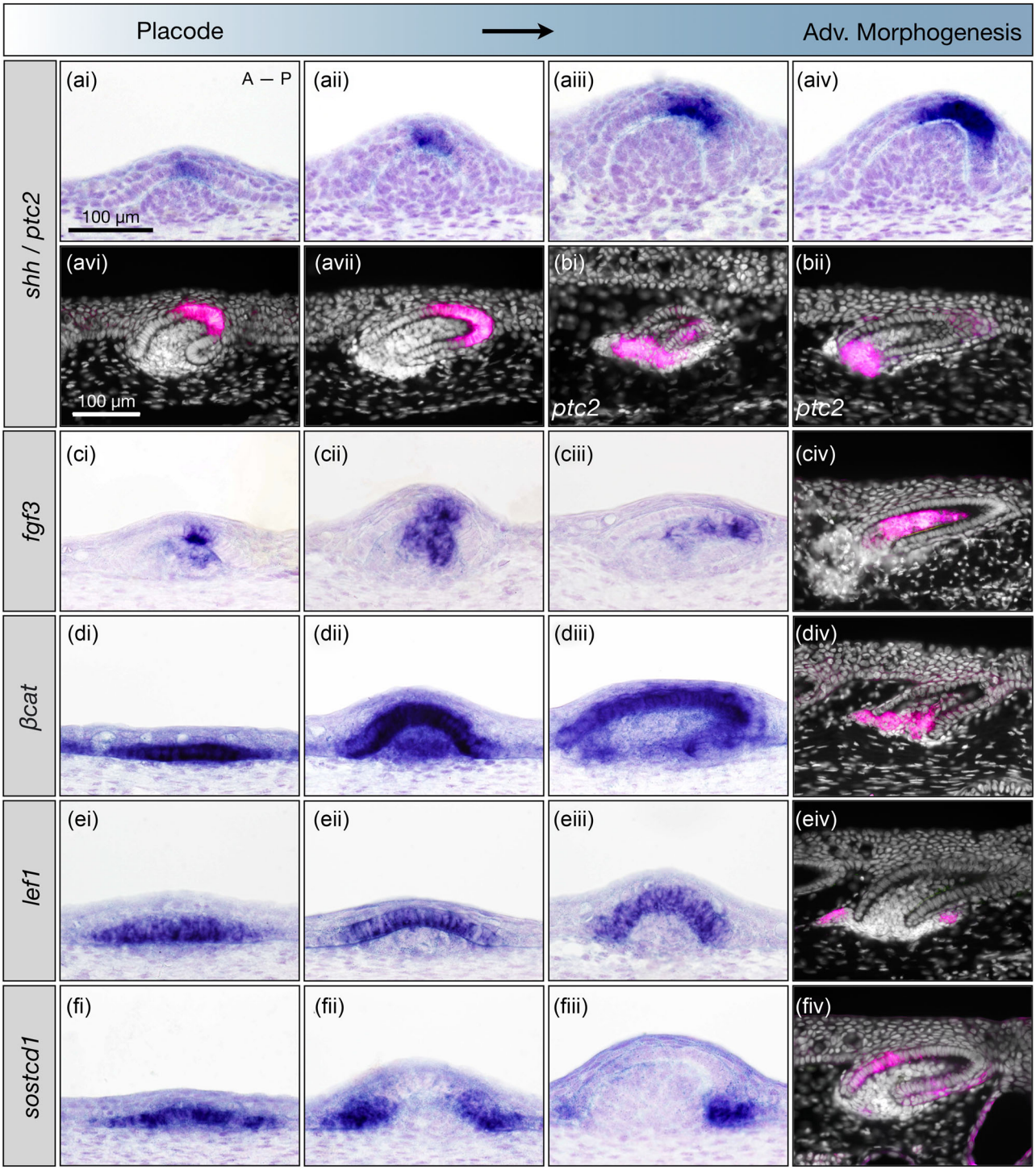

FIGURE 3 (See caption on next page)

the entire dental papilla (Figure 4aii). During later morphogenesis, expression in the distal epithelial tip increases (Figure 4aiii). Subsequent advanced morphogenesis is marked by maintenance of papillary expression, and a reduction in expression at the polarized epithelial tip (Figure 4aiv).

BMPs also regulate various aspects of tooth, feather, and hair follicle development by mediating epithelial-mesenchymal interactions (Åberg et al., 1997; Mou et al., 2011; Noramly & Morgan, 1998; Vainio et al., 1993). In particular, mesenchymal expression of *Bmp4* is highly conserved during skin appendage placode formation (Cooper et al., 2017; Di-Poï & Milinkovitch, 2016). In denticle development, *bmp4* is initially weakly expressed in the placode mesenchyme (Figure 4bi), with expression subsequently increasing in intensity as denticle outgrowth continues (Figure 4bii). Expression remains absent from the epithelium as morphogenesis progresses, marking the dermal papilla of the developing denticle (Figure 4biii). Later, this pattern is accompanied by epithelial expression at the cervical-loop-like basal regions of the denticle, equivalent to the cells at the junction between the inner and outer dental epithelium of developing teeth (IDE/ODE; Figure 4biv).

Of the Runt-related (Runx) family of transcription factors, *Runx2* is a major regulator of bone formation, regulating both the proliferation and differentiation of cells committed to osteoblastic lineages (Camilleri & Mcdonald, 2006). The deeply conserved odontogenic role of *runx2* has previously been shown by expression in both teeth and denticles of the catshark, implying its co-option from a common developmental module to allow the evolution of odontodes (Hecht et al., 2008). Here, we further investigate the expression patterns of *runx2* at various stages of denticle development. Expression is first detected in the mesenchyme underlying the early denticle placode (Figure 4ci). During subsequent bud outgrowth, this mesenchymal expression is maintained (Figure 4cii), however, expression subsequently spreads from the mesenchymal compartment into the directly overlying medial/apical epithelium (Figure 4ciii). In later stages of morphogenesis, expression becomes restricted to the basal mesenchyme of the advancing papilla and the surrounding deeply invaginated epithelial loops (equivalent to the dental cervical-loop-like regions; Figure 4civ).

The Twist transcription factor is also associated with bone development, via regulation of osteoblastic cell activity (Murray et al., 1992; Rice et al., 2000). Here, *twist* expression is first detected in the mesenchyme (Figure 4Di), in a comparable pattern to *runx2* (Figure 4ci). Further similarities with *runx2* are observed throughout placode outgrowth (Figure 4dii). During morphogenesis, however, *twist* shows restriction to the anterior aspect of the mesenchymal papilla, leaving an apparent negative region of posterior mesenchyme (Figure 4diii). By advanced stages of morphogenesis, *twist* becomes progressively restricted to the bilateral periphery of the basal mesenchyme of the papilla (Figure 4div) surrounding the epithelial cervical loop-like regions of the denticle (ODE/IDE equivalent cells).

The expression data presented here represents an initial framework for a hypothetical denticle gene regulatory network (dGRN) model, which shows broad conservation with the oral dentition, therefore expanding our knowledge of the conserved and ancient oGRN (Figure 4e) (Martin et al., 2016; Rasch et al., 2016, 2020). We observe the expression of several well-known tooth-related genes in an almost equivalent manner to early dental morphogenesis (Figures 3 and 4). We suggest that, whether odontodes first appeared in the oral/pharyngeal cavity or within the ectodermal epidermis, the oGRN likely emerged to form tooth-like structures before the

FIGURE 3 Gene expression patterns associated with shark denticle development. *shh* expression is observed in early developing denticles (a), increasing in intensity in the outgrowing cusp during morphogenesis and advanced morphogenesis (ai–avii). Expression of the Shh receptor, *ptch2*, is also noted in the basal mesenchyme directly underlying the papilla during morphogenesis (bi, bii). *fgf3* is first weakly expressed in the medial mesenchyme directly underlying the epithelial basal membrane (ci), before becoming restricted to an asymmetric region of the epithelium (cii, ciii). Strong *fgf3* expression is observed in the dermis during advanced morphogenesis (civ). Diffuse staining of *βcat* is observed in regions of the basal epithelium, marking placode initiation (di), and remains present during subsequent morphogenesis (dii, diii). By advanced morphogenesis, *βcat* is restricted to the basal mesenchyme of the papilla (div). During placode initiation, *lef1* is expressed in the basal epithelium (ei), and its expression is maintained throughout subsequent morphogenesis, before becoming restricted primarily to two bilateral regions of the basal mesenchyme adjacent to the papilla (eii, eiv). We also observed expression of *sostdc1* in the basal epithelium of each placode forming unit (fi), with expression becoming progressively restricted to the peripheral epithelium during subsequent morphogenesis, leaving a *sostcd1*-ve medial region (fii, fiv). False colored (magenta) images are counterstained with DAPI. The A–P axis refers to sample orientation, with A being anterior and P being posterior.

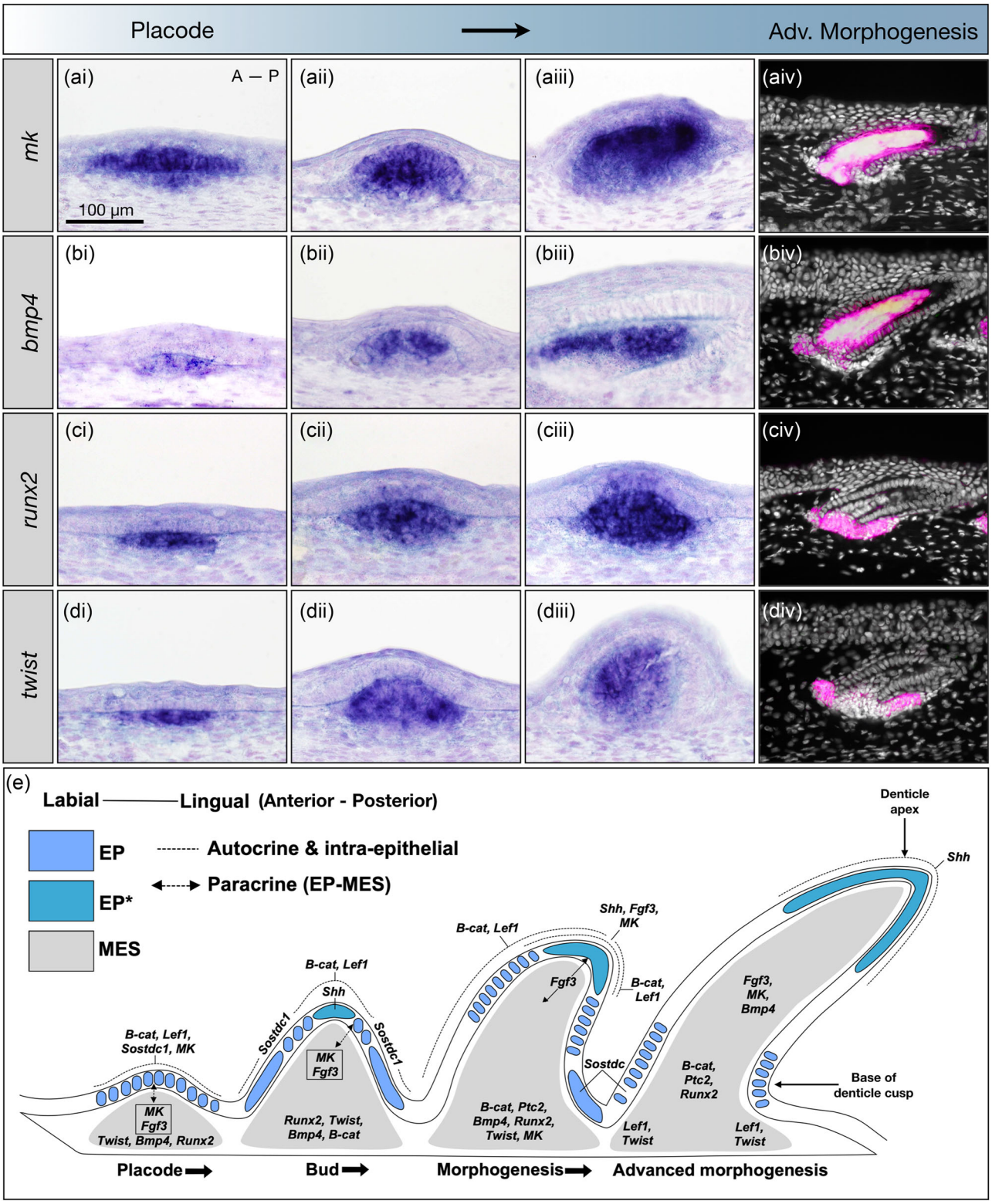

FIGURE 4 (See caption on next page)

evolution of true vertebrate teeth, and the mechanisms of tooth regeneration from within an active dental lamina likely evolved later.

3.4 | Shared gene expression patterns throughout oral tooth and dermal denticle development

Next, we undertook section *IS*H of the shark lower jaw, which contains both body denticles and teeth. This enabled us to examine patterns of simultaneous gene expression in these distinct odontode types (Figure 5).

In concurrence with our previous results (Figures 3 and 4), we observe conservation of gene expression patterns between both oral teeth and dermal denticles, including those of *βcat*, *lef1*, *fgf3*, *bmp4*, *sostdc1*, and *mk* (Figure 5a–f). However, although the transcription factor *sox2* is expressed in the developing dentition, it remains absent from the emerging denticles (Figure 5g) (Martin et al., 2016). We also note the expression of *sox2* in the developing regenerative taste buds (Figure 5h). This transcription factor has a conserved role related to the maintenance of the stem cell niche, essential for vertebrate tooth initiation and regeneration (Fraser et al., 2020; Juuri et al., 2013; Martin et al., 2016). This lack of expression in denticles may explain the difference in regenerative potential between these distinct odontode types. Finally, epithelial expression of *foxq1* was also observed simultaneously in both tooth morphogenesis and taste bud development (Figure 5i), and also in body denticle morphogenesis (Supporting Information: Figure S1).

3.5 | Tooth-associated gene expression patterns are deployed throughout development of the shark sensory system

Various sensory skin structures are located within close proximity of developing body denticles. Therefore, we next sought to compare the expression of several genes between emerging body denticles and other regenerative skin appendage types in the embryonic shark, including taste buds, pit organs, and ampullae of Lorenzini (Figure 6). Pit organs are defined here as nonampullae sensory pores that adorn the skin of sharks. In adult sharks, the opening of pit organs can exhibit an elongated morphology (Peach & Marshall, 2000), relative to the more circular pores of ampullae of Lorenzini (Peach & Marshall, 2000).

PCNA immunoreactivity of taste bud paraffin sections reveals outgrowth of a highly proliferative epithelial thickening (Figure 6ai). Interestingly, we also observe a medial zone of reduced proliferation throughout taste bud morphogenesis (Figure 6aii,iii), indicative of comparable proliferative growth to dorsal denticles (Figure 2). We also note similarities in specific gene expression patterns during taste bud morphogenesis. For example, *shh* expression is concentrated in the apical tip of the taste epithelium (Figure 6b), and *sostdc1* is restricted to lateral epithelial cells surrounding the apex of each taste bud (Figure 6c). *sox2* contributes to the development of various sensory structures (Castillo-Azofeifa et al., 2018; Martin et al., 2016; Okubo et al., 2006), and here we observe its expression in developing taste buds (Figure 6c) and the Ampullae of Lorenzini (Figure 6j). Conserved expression of *βcat* and *runx2* are also observed

FIGURE 4 Dermal gene expression patterns associated with shark denticle development. *mk* is strongly expressed in both the epithelium and underlying mesenchyme, from placode initiation through to advanced morphogenesis (ai–aiv). We also observe mesenchymal expression of *bmp4* (bi–biv), *runx2* (ci–civ), and *twist* (di–div) throughout dermal denticle development, from placode initiation to advanced morphogenesis. During advanced morphogenesis, *bmp4* expression highlights the entire dermal papilla (biv), whereas *runx2* and *twist* become restricted to the base of the outgrowing unit (div). False colored images are counterstained with DAPI. The A–P axis refers to sample orientation, with A being anterior and P being posterior. We also present a putative denticle GRN (e). We propose that molecular signaling cascades regulate denticle development from placode stage to advanced morphogenesis (from left to right; Anterior to Posterior), through expression of activators, inhibitors, polarizing growth signals and differentiation factors. *βcat* and *lef1* are proposed to positively regulate cell proliferation during development (Järvinen et al., 2006; Noramly et al., 1999), while inhibitors such as *sostdc1* and *bmp4* can precisely delineate these expression domains (Cho et al., 2011; Mou et al., 2011; Noramly & Morgan, 1998). Dynamic expression of *fgf3* and *mk* between the epithelium and mesenchyme suggests roles in mediating inductive tissue interactions (Kettunen et al., 2000; Mitsiadis et al., 2008). In association with *βcat*, progressive localization of *shh*, *fgf3*, and *mk* to the non-proliferative epithelial tip infers roles as polarizing factors, guiding unidirectional growth, and regulating subsequent cusp formation. This signaling center is proliferatively (Figure 2) and molecularly comparable to the mammalian enamel knot (Vaahtokari et al., 1996), which is also implicated in the development of dental cusps in elasmobranch teeth (Thiery et al., 2022). *Twist* is also proposed to act in accordance with its conserved role as a negative regulator of *runx2*, in advance of its function inducing cell differentiation for matrix deposition (Bialek et al., 2004). EP, epithelium; EP*, epithelial tip; MES, mesenchyme; EP-MES, epithelial-mesenchymal.

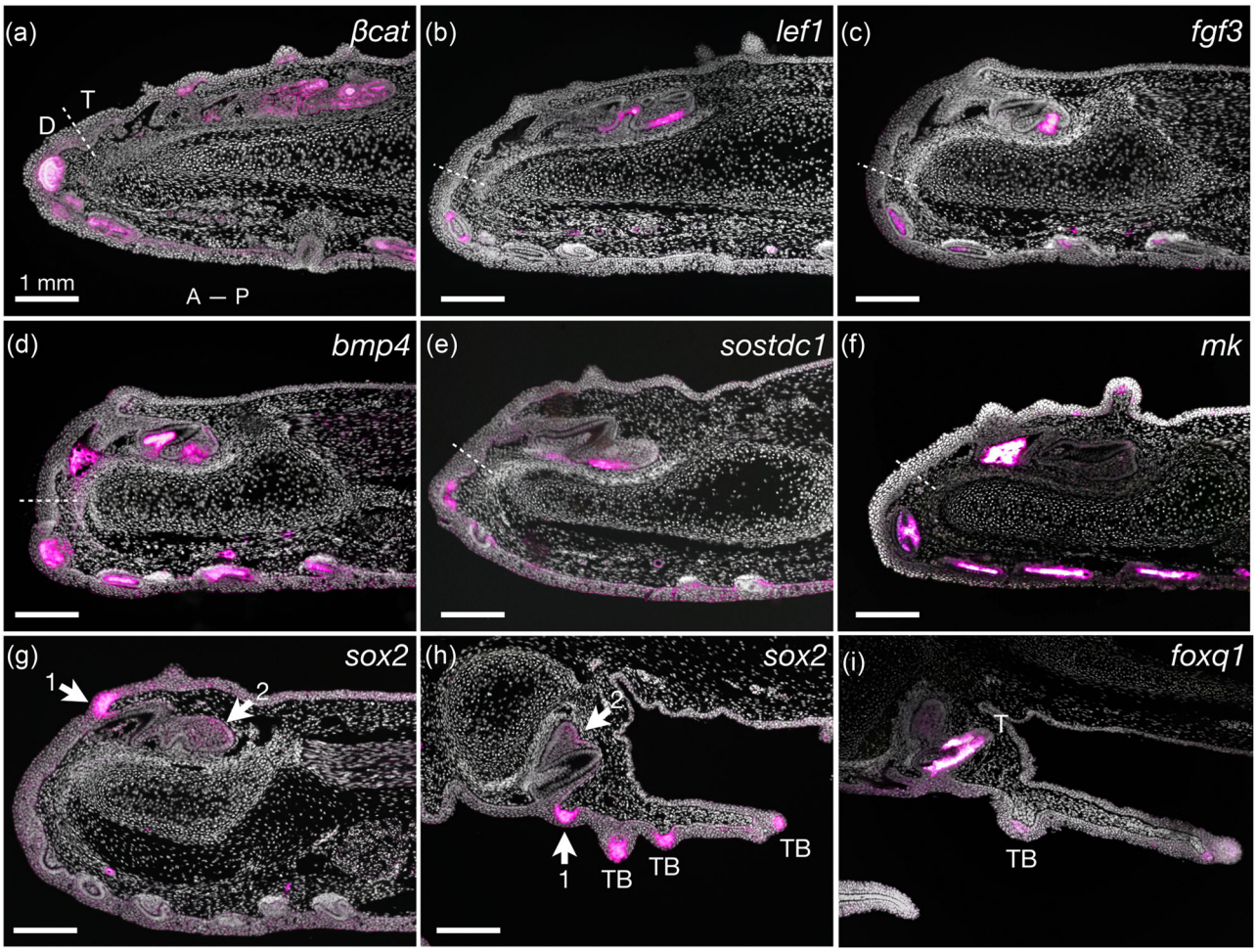

FIGURE 5 Gene expression patterns during development of both the regenerative shark dentition and the skin denticles. In both dermal denticles and oral teeth of the lower jaw at ~110 dpf (sagittal plane of section), simultaneously expressed genes imply the deployment of a common oGRN. In denticle and tooth development, commonly expressed *βcat*, *lef1*, *fgf3*, *bmp4*, *sostdc1*, and *mk* (a–f, respectively) define these key similarities, shown by their expression in both oral teeth and dermal denticles. Teeth (T) and denticles (D) are further demarcated by a putative boundary zone (dotted line) between the oral and dermal epithelia. Differential expression of *sox2*, confined to the dental lamina (g, h), provides a key difference between denticles and teeth. In the oral epithelium, *sox2* shows clear associations with developing teeth, where its expression marks a putative dental stem cell niche (g, arrow 1) linked with the successional lamina via a continuous epithelial stripe (h, arrow 2). Additionally, *sox2* marks regenerative taste buds (h, TB). This indicates a difference between inner (oral) and outer (dermal) epithelia, as defined by a *sox2*+ dental lamina that facilitates continuous tooth replacement, in contrast to *sox2*- dermal denticles, which do not exhibit a system of continuous replacement. Epithelial expression of *foxq1* was observed in developing teeth (i; T) within the inner dental epithelium at stages coincident with the secretory stages of the ameloblast. Expression of *foxq1* is also present in the epithelial components of the tastebuds (TB) located on the medial valve of the inner upper jaw. The A–P axis refers to sample orientation, with A being anterior and P being posterior.

(Figure 6e,f). Additionally, we observe expression of Fox gene family member, *foxq1*, a known inducer of epithelial differentiation, during shark taste bud development (Figure 6g) (Feuerborn et al., 2011). *βcat* and *mk* are also present during pit organ development (Figure 6h,i). Overall, we observe broad conservation of tooth-related gene expression patterns during the early development of the shark sensory system.

3.6 | Conserved gene expression patterns are deployed during the early development of both shark denticles and avian feathers

Having observed similarities between expression patterns of tooth-related genes throughout development of both denticles and the shark sensory system, we next sought

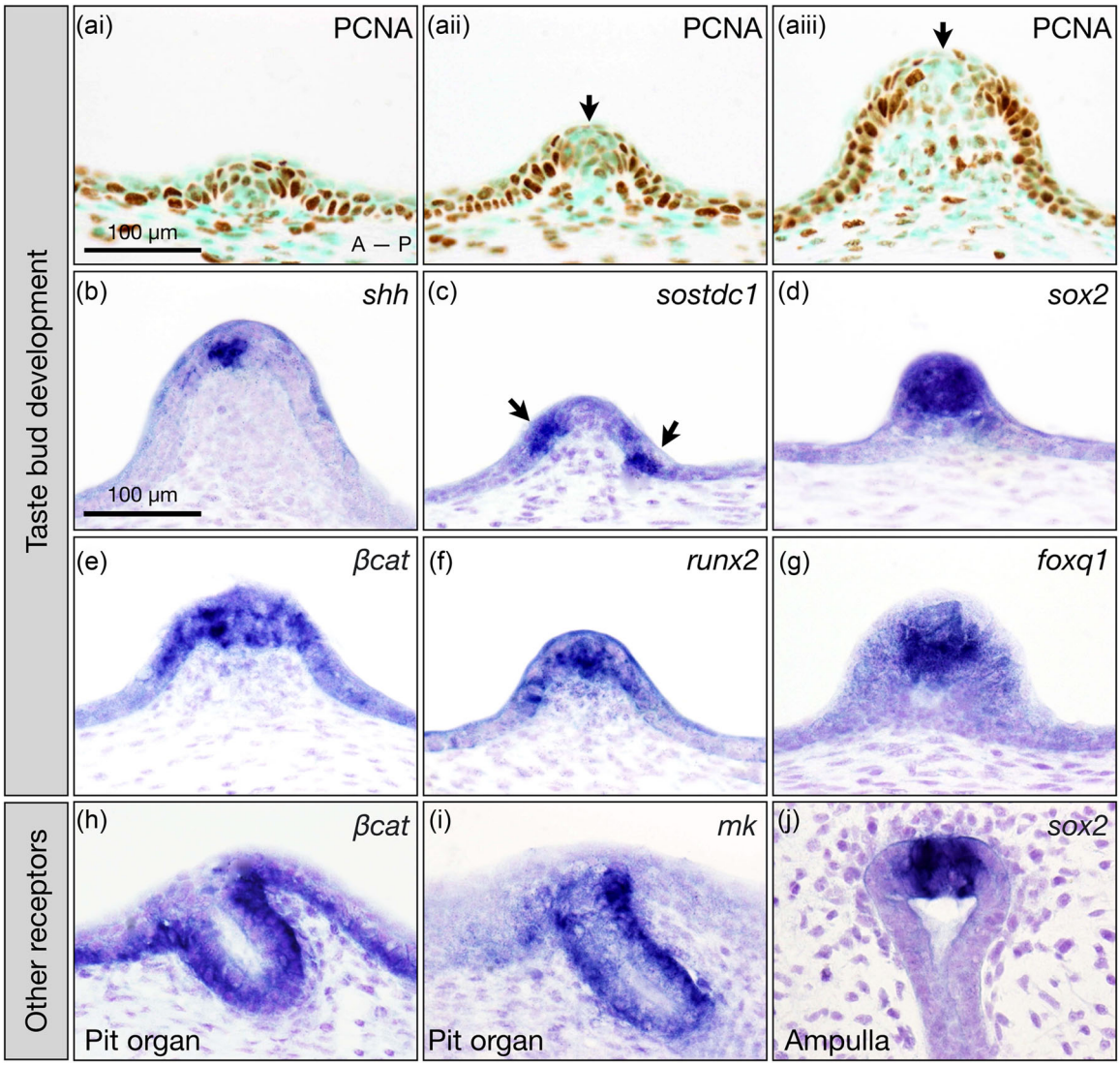

FIGURE 6 Cell proliferation and conserved gene expression patterns associated with the development of sensory receptors in the shark. Proliferating cell nuclear antigen (PCNA) immunoreactivity reveals that taste bud papillae arise through controlled proliferation of the epithelium from the placode stage (ai) to later morphogenesis (aii, aiii). Reduced proliferation in the papillae tip is also noted here (aii, aiii, black arrow). At similar stages, *shh* is expressed in the evaginating epidermis (b). At preceding stages, *sostdc1* is expressed bilaterally in the periphery of early taste bud papillae (c, arrows). Additional markers, including *sox2*, *βcat*, *runx2*, and *foxq1* (d–g) are expressed in the epithelium at various developmental stages. Additionally, *βcat* and *mk* are also expressed in developing pit organs, and *sox2* can be observed in the sensory cells of the Ampullae of Lorenzini. The A–P axis refers to sample orientation, with A being anterior and P being posterior.

to examine whether this conservation extends beyond sharks, to encompass the skin appendages of other species. Previous research has demonstrated that the anatomical placode constitutes a common foundation from which diverse skin appendages are derived across phylogenetically distinct vertebrate groups (Cooper et al., 2017; Di-Poï & Milinkovitch, 2016; Harris et al., 2008). Using whole mount *IS*H, we compared expression patterns of conserved developmental genes during skin appendage development of both the shark and the chicken embryo (Figure 7).

As previously noted from section *IS*H (Figure 3a), whole mount *IS*H reveals that expression of *shh* is restricted to the posterior facing apex of denticles undergoing morphogenesis (Figure 7a). Conversely, expression of both *fgf4* and *bmp4* appears restricted to the mesenchymal papilla of the developing denticle, located behind the apical *shh* signal (Figure 3b,c)

(Cooper et al., 2018). Immunofluorescence reveals medial localization of Shh in the denticle placode, within a highly proliferative epithelium (Figure 7d). Comparable expression patterns are also observed in the chicken embryo, with feather buds expressing apically concentrated *Shh*, and dermal expression of both *Fgf4* and *Bmp4* within the feather bud papilla (Figure 7e–g) (Jung et al., 1998). Here, immunofluorescence reveals an accumulation of Shh at the feather bud edge (Figure 7h), potentially contributing to polarized outgrowth. Overall, we observe notable similarity of gene expression patterns during the early development of both shark denticles and chicken feathers, indicating that the conserved putative oGRN proposed here (Martin et al., 2016) is likely present across the skin appendages of phylogenetically distinct vertebrates.

4 | DISCUSSION

This study has revealed several findings regarding the development of shark dermal denticles. First, during denticle development, many genes associated with tooth development are expressed in domains comparable to

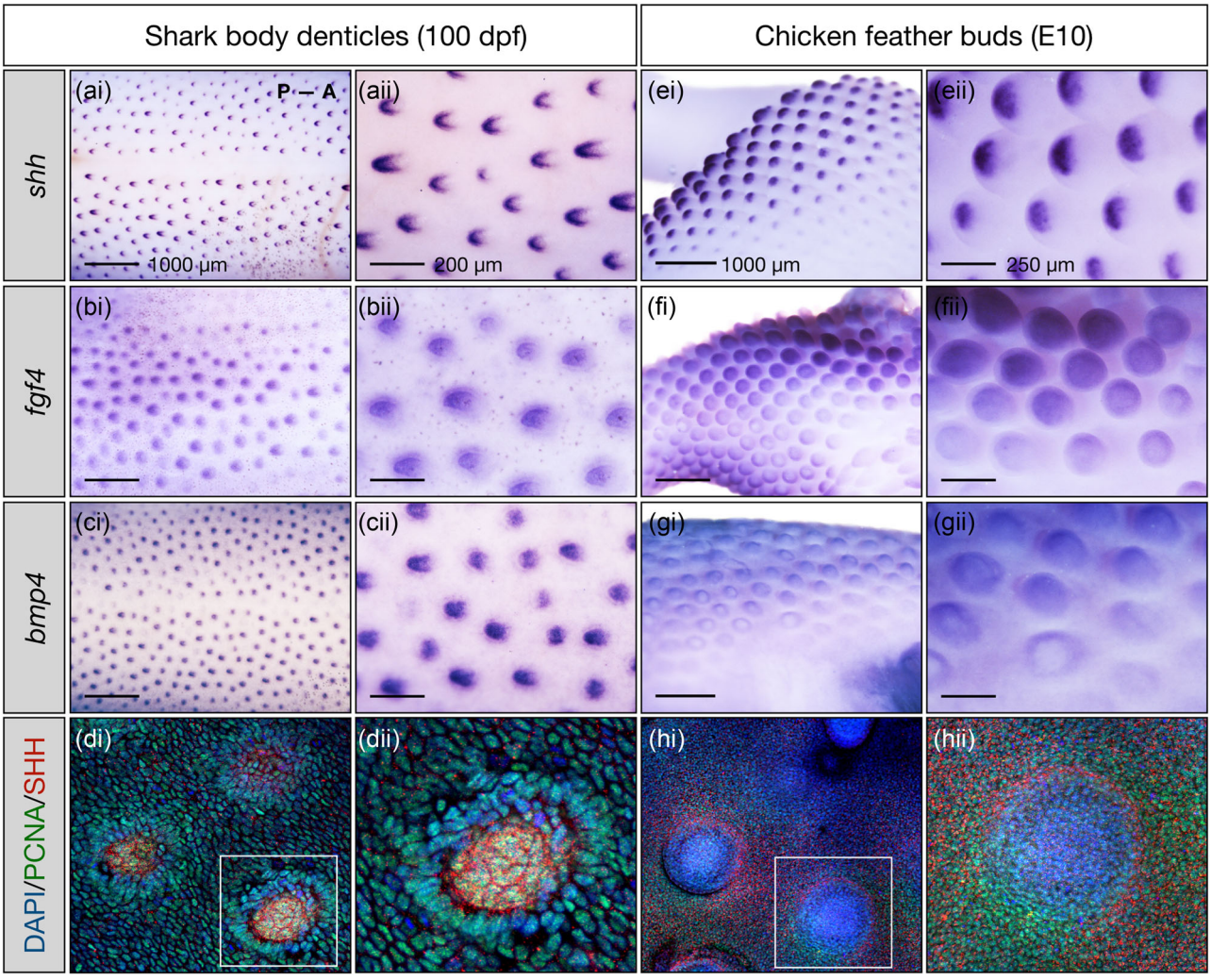

FIGURE 7 Conserved gene expression patterns during early shark denticle and avian feather development. The early development (patterning and early morphogenesis) of shark denticles and chicken feathers is compared, using whole mount in situ hybridisation (ISH). The early development of shark body denticles is observed at 100 dpf (a–d). Epithelial expression of *shh* is observed in the posterior cusp of developing denticles (a), whereas *fgf4* and *bmp4* expression is observed more centrally, in the underlying mesenchyme (b,c) (Cooper et al., 2018). Whole mount immunofluorescence revealed medial local expression of SHH associated with proliferative denticle placodes (d). As previously shown, chicken feather buds display comparable patterns of gene expression at E10 (e–h) (Jung et al., 1998; Noramly et al., 1999), with epithelial expression of *Shh* in the leading tip of the feather bud (e), and dermal expression of both *fgf4* and *bmp4* (f–g) (Jung et al., 1998). Anti-SHH is also observed localized to individual developing feather buds (h). The P–A axis refers to sample orientation, with A being anterior and P being posterior.

developing teeth, indicating that a conserved oGRN regulates the development of both of these skin appendages (Martin et al., 2016). This is particularly apparent in the epithelial tip of the denticle (apical epithelial knot: AEK; Thiery et al., 2022), which, in common with the shark dentition, shows reduced cell proliferation accompanied by expression of *shh*, *fgf3*, and *mk* (Figure 3). This provides further evidence to support the ancestral conservation of a modular cusp-making signaling center analogous to the mammalian enamel knot (Thiery et al., 2022). This study therefore reveals a significant degree of conservation regarding the morphogenesis of both denticles and teeth.

Furthermore, our comparison of spatial gene expression patterns between the oral teeth and dermal denticles of sharks has implications for current models of odontode evolution. With the expression of identical genes observed between both oral teeth, which develop within a dental lamina, and external skin denticles (Figure 5), our findings support the "inside and out" hypothesis model of tooth origins, suggesting the simultaneous deployment of a shared and co-opted odontode gene regulatory network (oGRN) (Donoghue & Rücklin, 2016; Fraser et al., 2010; Martin et al., 2016; Smith & Coates, 1998). Although our study is not intended to provide a framework for elucidating the origins of teeth, these data expand our knowledge of a shared and equivalent odontode-related genetic toolkit.

A notable difference between dermal denticles and oral teeth in sharks is the differential expression of *sox2* (Figure 5), restricted exclusively in the dentition, to the cells of the dental lamina that contribute to the early dental epithelium and dental stem cell niche (Martin et al., 2016). This discrepancy underlies the difference in regenerative potential between the oral and dermal epithelia, with oral teeth exhibiting a continuous replacement system, in contrast to dermal denticles, which show no obvious corresponding evidence of autonomous renewal (Martin et al., 2016). Although our findings generally conform to a proposed system of common odontogenic potential in both the oral and dermal epithelia, this differential expression of *sox2* is indicative of a divergence in the shared oGRN (Donoghue & Rücklin, 2016; Smith & Coates, 1998). Dermal denticles can regenerate following wounding, although secondary units do not retain their original orientation or patterning (Reif, 1978). In contrast to shark tooth replacement, the molecular circuitry that underpins denticle replacement appears to lack a stepwise, continuous pattern of epithelial expression from lamina-like epithelial cells. However, there are reports that denticles are replaced overtime, for example in the Thresher shark (*Alopias vulpinus*) several "gaps" are observed on the surface of tail with some evidence of denticles growing from within the skin below these gaps (Popp et al., 2020). These recent data suggest that denticles exhibit a generational replacement mechanism. A closer examination of the developmental time sequence and the related molecular shifts throughout the life-cycle of individual denticles, and the response to regeneration following wounding, would provide an interesting comparison to the better understand the system of continuous tooth replacement (Martin et al., 2016; Rasch et al., 2016)

An interesting observation is the expression of common genes during both tooth and denticle development are also observed in the development of neighboring elasmobranch sensory receptors. This highlights shared, primitive features of these disparate skin appendages, expanding our understanding of the conservation of genes in neighboring epithelial units and potentially providing a basis for further discussions of evolutionary origin of teeth and tooth-like structures (Donoghue, 2002). This conforms to the "inside and out" model which postulates that teeth and denticles may be derived from the cooperation of tissues associated with precursory epithelial units, perhaps regenerative with a sensory function, and a newly acquired neural crest-derived cell type, which together developed odontogenic potential (Baker & Bronner-Fraser, 1997; Fraser et al., 2010). Progressive remodulation of common signals may have led to the appearance and subsequent diversification of teeth and denticles (Fraser et al., 2010). Furthermore, in concurrence with previous research (Cooper et al., 2017; Di-Poï & Milinkovitch, 2016; Harris et al., 2008), our comparison of denticle and feather development (Figure 7) demonstrates that the conservation of placode initiation and early morphogenesis is observed not only between the shark sensory system and odontodes, but also across skin appendages of phylogenetically distinct vertebrates. Later divergence in developmental processes then gives rise to the plethora of diverse skin appendages observed in nature.

We have characterized and compared the molecular development of odontodes in the shark (Figures 3–5). However, there is growing evidence to suggest that, in addition to genetic regulation, mechanical systems are also paramount in controlling skin appendage development (Shyer et al., 2013, 2017). This includes processes such as mechanosensation resulting from cellular aggregation, which can initiate genetic signaling cascades (Ho et al., 2019). In fact, integrated molecular and mechanical systems are known to control the precise patterning of the feather array in avian species (Ho et al., 2019). To obtain a comprehensive understanding of both the physical and molecular systems at play during the

development of both shark denticles and teeth, such mechanical processes should also be investigated in future studies. This will provide evolutionary perspectives regarding the emergence of such mechanical systems in the context of skin appendage development.

5 | CONCLUSIONS

Here, we have charted the development of dermal denticles, comparing conserved gene expression patterns with those of the developing shark dentition. This has revealed shared developmental gene expression across both shark denticles and sensory receptors, suggesting a common GRN might operate during the evolution and development of all skin appendages of epithelial origin. We predict that an ancient odontode, at the advent of vertebrates, would have employed this same, common set of genes during emergence from the skin. Patterns of both cell proliferation and specific gene signaling during placode initiation and subsequent morphogenesis imply the presence of a modular signaling center comparable to the mammalian enamel knot (EK) (Vaahtokari et al., 1996), and the apical epithelial knot (AEK) in sharks (Thiery et al., 2022). Integration of these gene expression patterns with additional markers from tooth development add to the wider putative ancestral oGRN model (Figure 4e) (Martin et al., 2016; Rasch et al., 2016). This generally conforms to the "inside and out" model of tooth origin, which views the development of teeth and denticles as conserved at the molecular level (Fraser et al., 2010; Smith & Coates, 1998). However, the differential expression of the dental stem cell marker *sox2*, restricted to the epithelia of the oral dentition, implies a key difference in odontode initiation and regenerative potential between oral and epidermal locations. Future studies including RNA-sequencing will yield a more comprehensive understanding of the common and differential molecular signature of development in both dermal denticles and oral teeth, and will elucidate how differential gene expression patterns are related to variation in their regenerative capacities, but also variation in their supporting tissue and attachment mechanisms.

ACKNOWLEDGMENTS

We thank the anonymous reviewers for their time and comments on previous versions of the manuscript. Additionally, we thank Alexandre Thiery, and past and present members of the Fraser Lab for stimulating discussion associated with this project. We also extend our gratitude to Kyle Martin, Zerina Johanson (Department of Earth Sciences, Natural History Museum, London), Farah Ahmed, and Armin Garbout (Imaging and Analysis Center, Natural History Museum, London) for assistance with micro-CT imaging. This research was supported by the following research grants: National Science Foundation IntBIO Collaborative Research grant: 2128032 (to Gareth J. Fraser); Natural Environment Research Council (NERC) Standard Grant NE/K014595/1 (to Gareth J. Fraser); NERC PhD studentship (to Liam J. Rasch), and Leverhulme Trust Research Grant RPG-211 (to Gareth J. Fraser). This work was also funded through "Adapting to the Challenges of a Changing Environment" (ACCE), a NERC-funded doctoral training partnership (to Rory L. Cooper) ACCE DTP (NE/L002450/1). The authors declare that they have no conflict of interest.

DATA AVAILABILITY STATEMENT

The data that support the findings of this study are available from the corresponding author upon reasonable request.

ORCID

Rory L. Cooper http://orcid.org/0000-0003-0172-4708
Gareth J. Fraser http://orcid.org/0000-0002-7376-0962

REFERENCES

Åberg, T., Wozney, J., & Thesleff, I. (1997). Expression patterns of bone morphogenetic proteins (Bmps) in the developing mouse tooth suggest roles in morphogenesis and cell differentiation. *Developmental Dynamics*, *210*, 383–396.

Ahn, Y., Sanderson, B. W., Klein, O. D., & Krumlauf, R. (2010). Inhibition of Wnt signaling by wise (Sostdc1) and negative feedback from Shh controls tooth number and patterning. *Development*, *137*, 3221–3231.

Baker, C. V., & Bronner-Fraser, M. (1997). The origins of the neural crest. *Mechanisms of Development*, *69*, 3–11.

Ballard, W., Mellinger, J., & Lechenault, H. (1993). A series of normal stages for development of *Scyliorhinus canicula*, the Lesser spotted dogfish (Chondrichthyes: Scyliorhinidae). *The Journal of Experimental Zoology*.

Bei, M., & Maas, R. (1998). FGFs and BMP4 induce both Msx1-independent and Msx1-dependent signaling pathways in early tooth development. *Development*, *125*, 4325–4333.

Bialek, P., Kern, B., Yang, X., Schrock, M., Sosic, D., Hong, N., Wu, H., Yu, K., Ornitz, D. M., Olson, E. N., Justice, M. J., & Karsenty, G. (2004). A twist code determines the onset of osteoblast differentiation. *Developmental Cell*, *6*, 423–435.

Busby, L., Aceituno, C., Mcqueen, C., Rich, C. A., Ros, M. A., & Towers, M. (2020). Sonic hedgehog specifies flight feather positional information in avian wings. *Development*, *147*, 1–11.

Camilleri, S., & Mcdonald, F. (2006). Runx2 and dental development. *European Journal of Oral Sciences*, *114*, 361–373.

Castillo-Azofeifa, D., Seidel, K., Gross, L., Golden, E. J., Jacquez, B., Klein, O. D., & Barlow, L. A. (2018). SOX2 regulation by hedgehog signaling controls adult lingual epithelium homeostasis. *Development*, *145*(14), 1–13.

Chen, D., Blom, H., Sanchez, S., Tafforeau, P., Märss, T., & Ahlberg, P. E. (2020). The developmental relationship between teeth and dermal odontodes in the most primitive bony fish Lophosteus. *eLife*, *9*, e60985.

Chen, D., Jarrell, A., Guo, C., Lang, R., & Atit, R. (2012). Dermal β-catenin activity in response to epidermal Wnt ligands is required for fibroblast proliferation and hair follicle initiation. *Development (Cambridge, England)*, *139*(8), 1522–1533.

Chen, J., Lan, Y., Baek, J. A., Gao, Y., & Jiang, R. (2009). Wnt/beta-catenin signaling plays an essential role in activation of odontogenic mesenchyme during early tooth development. *Developmental Biology*, *334*, 174–185.

Chiang, C., Swan, R. Z., Grachtchouk, M., Bolinger, M., Litingtung, Y., Robertson, E. K., Cooper, M. K., Gaffield, W., Westphal, H., Beachy, P. A., & Dlugosz, A. A. (1999). Essential role for sonic hedgehog during hair follicle morphogenesis. *Developmental Biology*, *205*, 1–9.

Cho, S.-W., Kwak, S., Woolley, T. E., Lee, M.-J., Kim, E.-J., Baker, R. E., Kim, H.-J., Shin, J.-S., Tickle, C., Maini, P. K., & Jung, H.-S. (2011). Interactions between Shh, Sostdc1 and Wnt signaling and a new feedback loop for spatial patterning of the teeth. *Development (Cambridge, England)*, *138*(9), 1807–1816.

Chuong, C. M., Patel, N., Lin, J., Jung, H. S., & Widelitz, R. B. (2000). Sonic hedgehog signaling pathway in vertebrate epithelial appendage morphogenesis: Perspectives in development and evolution. *Cellular and Molecular Life Sciences*, *57*, 1672–1681.

Cooper, R. L., Lloyd, V. J., Di-Poï, N., Fletcher, A. G., Barrett, P. M., & Fraser, G. J. (2019). Conserved gene signalling and a derived patterning mechanism underlie the development of avian footpad scales. *EvoDevo*, *10*, 19.

Cooper, R. L., Martin, K. J., Rasch, L. J., & Fraser, G. J. (2017). Developing an ancient epithelial appendage: FGF signalling regulates early tail denticle formation in sharks. *EvoDevo*, *8*, 8.

Cooper, R. L., Thiery, A. P., Fletcher, A. G., Delbarre, D. J., Rasch, L. J., & Fraser, G. J. (2018). An ancient turing-like patterning mechanism regulates skin denticle development in sharks. *Science Advances*, *4*, eaau5484.

Debiais-Thibaud, M., Chiori, R., Enault, S., Oulion, S., Germon, I., Martinand-Mari, C., Casane, D., & Borday-Birraux, V. (2015). Tooth and scale morphogenesis in shark: An alternative process to the mammalian enamel knot system. *BMC Evolutionary Biology*, *15*, 292.

Debiais-Thibaud, M., Oulion, S., Bourrat, F., Laurenti, P., Casane, D., & Borday-Birraux, V. (2011). The homology of odontodes in gnathostomes: Insights from Dlx gene expression in the dogfish, *Scyliorhinus canicula*. *BMC Evolutionary Biology*, *11*, 307.

Di-Poï, N., & Milinkovitch, M. C. (2016). The anatomical placode in reptile scale morphogenesis indicates shared ancestry among skin appendages in amniotes. *Science Advances*, *2*, e1600708.

Donoghue, P. C. J. (2002). Evolution of development of the vertebrate dermal and oral skeletons: Unraveling concepts. regulatory theories and homologies. *Palaeobiology 28*(4), 474–507.

Donoghue, P. C. J., & Rücklin, M. (2016). The ins and outs of the evolutionary origin of teeth. *Evolution & Development*, *18*(1), 19–30.

Enault, S., Adnet, S., & Debiais-Thibaud, M. (2016). Skeletogenesis during the late embryonic development of the catshark *Scyliorhinus canicula* (Chondrichthyes; Neoselachii). *MorphoMuseuM*, *1*, e2.

Feuerborn, A., Srivastava, P. K., Küffer, S., Grandy, W. A., Sijmonsma, T. P., Gretz, N., Brors, B., & Gröne, H. J. (2011). The Forkhead factor FoxQ1 influences epithelial differentiation. *Journal of Cellular Physiology*, *226*, 710–719.

Fraser, G. J., Bloomquist, R. F., & Streelman, J. T. (2013). Common developmental pathways link tooth shape to regeneration. *Developmental Biology*, *377*, 399–414.

Fraser, G. J., Cerny, R., Soukup, V., Bronner-Fraser, M., & Streelman, J. T. (2010). The odontode explosion: The origin of tooth-like structures in vertebrates. *BioEssays*, *32*, 808–817.

Fraser, G. J., Standing, A., Underwood, C., & Thiery, A. P. (2020). The dental lamina: An essential structure for perpetual tooth regeneration in sharks. *Integrative and Comparative Biology*, *60*, 644–655.

Gabler-Smith, M. K., Wainwright, D. K., Wong, G. A., & Lauder, G. V. (2021). Dermal denticle diversity in sharks: Novel patterns on the interbranchial skin. *Integrative Organismal Biology*, *3*, obab034.

Gillis, J. A., & Donoghue, P. C. J. (2007). The homology and phylogeny of chondrichthyan tooth enameloid. *Journal of Morphology*, *268*, 33–49.

Gillis, J. A., Rawlinson, K. A., Bell, J., Lyon, W. S., Baker, C. V. H., & Shubin, N. H. (2011). Holocephalan embryos provide evidence for gill arch appendage reduction and opercular evolution in cartilaginous fishes. *Proceedings of the National Academy of Sciences*, *108*, 1507–1512.

Handrigan, G. R., & Richman, J. M. (2010). A network of Wnt, hedgehog and BMP signaling pathways regulates tooth replacement in snakes. *Developmental Biology*, *348*, 130–141.

Harris, M. P., Rohner, N., Schwarz, H., Perathoner, S., Konstantinidis, P., & Nüsslein-Volhard, C. (2008). Zebrafish eda and edar mutants reveal conserved and ancestral roles of ectodysplasin signaling in vertebrates. *PLoS Genetics*, *4*, e1000206.

Hecht, J., Stricker, S., Wiecha, U., Stiege, A., Panopoulou, G., Podsiadlowski, L., Poustka, A. J., Dieterich, C., Ehrich, S., Suvorova, J., Mundlos, S., & Seitz, V. (2008). Evolution of a core gene network for skeletogenesis in chordates. *PLoS Genetics*, *4*, e1000025.

Ho, W. K. W., Freem, L., Zhao, D., Painter, K. J., Woolley, T. E., Gaffney, E. A., Mcgrew, M. J., Tzika, A., Milinkovitch, M. C., Schneider, P., Drusko, A., Matthäus, F., Glover, J. D., Wells, K. L., Johansson, J. A., Davey, M. G., Sang, H. M., Clinton, M., & Headon, D. J. (2019). Feather arrays are patterned by interacting signalling and cell density waves. *PLoS Biology*, *17*, e3000132.

Ingham, P. W., & Mcmahon, A. P. (2001). Hedgehog signaling in animal development: Paradigms and principles. *Genes & Development*, *15*, 3059–3087.

Jackman, W. R., Draper, B. W., & Stock, D. W. (2004). Fgf signaling is required for zebrafish tooth development. *Developmental Biology*, *274*, 139–157.

Järvinen, E., Salazar-Ciudad, I., Birchmeier, W., Taketo, M. M., Jernvall, J., & Thesleff, I. (2006). Continuous tooth generation in mouse is induced by activated epithelial Wnt/β-catenin signaling. *Proceedings of the National Academy of Sciences*, *103*, 18627–18632.

Jernvall, J., & Thesleff, I. (2000). Reiterative signaling and patterning during mammalian tooth morphogenesis. *Mechanisms of Development*, *92*, 19–29.

Jernvall, J., & Thesleff, I. (2012). Tooth shape formation and tooth renewal: Evolving with the same signals. *Development*, *139*, 3487–3497.

Johanson, Z., Smith, M. M., & Joss, J. M. P. (2007). Early scale development in heterodontus (Heterodontiformes; Chondrichthyes): A novel chondrichthyan scale pattern: Novel chondrichthyan scale pattern • Johansonet al. *Acta Zoologica*, *88*, 249–256.

Johanson, Z., Tanaka, M., Chaplin, N., & Smith, M. (2008). Early palaeozoic dentine and patterned scales in the embryonic catshark tail. *Biology Letters*, *4*, 87–90.

Jung, H.-S., Francis-West, P. H., Widelitz, R. B., Jiang, T.-X., Ting-Berreth, S., Tickle, C., Wolpert, L., & Chuong, C.-M. (1998). Local inhibitory action of BMPs and their relationships with activators in feather formation: Implications for periodic patterning. *Developmental Biology*, *196*, 11–23.

Juuri, E., Jussila, M., Seidel, K., Holmes, S., Wu, P., Richman, J., Heikinheimo, K., Chuong, C.-M., Arnold, K., Hochedlinger, K., Klein, O., Michon, F., & Thesleff, I. (2013). Sox2 marks epithelial competence to generate teeth in mammals and reptiles. *Development*, *140*, 1424–1432.

Kettunen, P., Laurikkala, J., Itäranta, P., Vainio, S., Itoh, N., & Thesleff, I. (2000). Associations of FGF-3 and FGF-10 with signaling networks regulating tooth morphogenesis. *Developmental Dynamics*, *219*, 322–332.

Kondo, S. (2002). The reaction-diffusion system: A mechanism for autonomous pattern formation in the animal skin. *Genes to Cells*, *7*, 535–541.

Mandler, M., & Neubüser, A. (2004). FGF signaling is required for initiation of feather placode development. *Development*, *131*, 3333–3343.

Martin, K. J., Rasch, L. J., Cooper, R. L., Metscher, B. D., Johanson, Z., & Fraser, G. J. (2016). Sox2+ progenitors in sharks link taste development with the evolution of regenerative teeth from denticles. *Proceedings of the National Academy of Sciences*, *113*, 14769–14774.

Millar, S. E., Willert, K., Salinas, P. C., Roelink, H., Nusse, R., Sussman, D. J., & Barsh, G. S. (1999). WNT signaling in the control of hair growth and structure. *Developmental Biology*, *207*(1), 133–149.

Mitsiadis, T. A., Caton, J., De Bari, C., & Bluteau, G. (2008). The large functional spectrum of the heparin-binding cytokines MK and HB-GAM in continuously growing organs: The rodent incisor as a model. *Developmental Biology*, *320*, 256–266.

Mitsiadis, T. A., Muramatsu, T., Muramatsu, H., & Thesleff, I. (1995). Midkine (MK), a heparin-binding growth/differentiation factor, is regulated by retinoic acid and epithelial-mesenchymal interactions in the developing mouse tooth, and affects cell proliferation and morphogenesis. *Journal of Cell Biology*, *129*, 267–281.

Mori, S., & Nakamura, T. (2022). Redeployment of odontode gene regulatory network underlies dermal denticle formation and evolution in suckermouth armored catfish. *Scientific Reports*, *12*, 6172.

Motta, P., Habegger, M. L., Lang, A., Hueter, R., & Davis, J. (2012). Scale morphology and flexibility in the shortfin mako *Isurus oxyrinchus* and the blacktip shark *Carcharhinus limbatus*. *Journal of Morphology*, *273*, 1096–1110.

Mou, C., Pitel, F., Gourichon, D., Vignoles, F., Tzika, A., Tato, P., Yu, L., Burt, D. W., Bed'hom, B., Tixier-Boichard, M., Painter, K. J., & Headon, D. J. (2011). Cryptic patterning of avian skin confers a developmental facility for loss of neck feathering. *PLoS Biology*, *9*, e1001028.

Munne, P. M., Tummers, M., Järvinen, E., Thesleff, I., & Jernvall, J. (2009). Tinkering with the inductive mesenchyme: Sostdc1 uncovers the role of dental mesenchyme in limiting tooth induction. *Development*, *136*, 393–402.

Murdock, D. J. E., Dong, X. P., Repetski, J. E., Marone, F., Stampanoni, M., & Donoghue, P. C. J. (2013). The origin of conodonts and of vertebrate mineralized skeletons. *Nature*, *502*, 546–549.

Murray, S. S., Glackin, C. A., Winters, K. A., Gazit, D., Kahn, A. J., & Murray, E. J. (1992). Expression of helix-loop-helix regulatory genes during differentiation of mouse osteoblastic cell. *Journal of Bone and Mineral Research*, *7*, 1131–1138.

Noramly, S., Freeman, A., & Morgan, B. A. (1999). β-catenin signaling can initiate feather bud development. *Development*, *126*(16), 3509–3521.

Noramly, S., & Morgan, B. A. (1998). BMPs mediate lateral inhibition at successive stages in feather tract development. *Development (Cambridge, England)*, *125*(19), 3775–3787.

Oeffner, J., & Lauder, G. V. (2012). The hydrodynamic function of shark skin and two biomimetic applications. *Journal of Experimental Biology*, *215*, 785–795.

Okubo, T., Pevny, L. H., & Hogan, B. L. M. (2006). Sox2 is required for development of taste bud sensory cells. *Genes & Development*, *20*, 2654–2659.

Ørvig, T. (1977). A survey of odontodes ('dermal teeth') from developmental, structural, functional and phyletic points of view. In S. M. Andrews, R. S. Miles, & A. D. Walker (Eds.), *Problems in Vertebrate Evolution, Linnean. Society Symposium Series 4* (pp. 53–75). Academis Press.

Park, Y. H., Lee, Y. S., Seo, Y. M., Seo, H., Park, J. S., Bae, H. S., & Park, J. C. (2020). Midkine promotes odontoblast-like differentiation and tertiary dentin formation. *Journal of Dental Research*, *99*, 1082–1091.

Peach, M. B., & Marshall, N. J. (2000). The pit organs of elasmobranchs: A review. *Philosophical Transactions of the Royal Society of London. Series B: Biological Sciences*, *355*, 1131–1134.

Popp, M., White, C. F., Bernal, D., Wainwright, D. K., & Lauder, G. V. (2020). The denticle surface of thresher shark tails: Three-dimensional structure and comparison to other pelagic species. *Journal of Morphology*, *281*, 938–955.

Rasch, L. J., Cooper, R. L., Underwood, C., Dillard, W. A., Thiery, A. P., & Fraser, G. J. (2020). Development and regeneration of the crushing dentition in skates (Rajidae). *Developmental Biology*, *466*, 59–72.

Rasch, L. J., Martin, K. J., Cooper, R. L., Metscher, B. D., Underwood, C. J., & Fraser, G. J. (2016). An ancient dental gene set governs development and continuous regeneration of teeth in sharks. *Developmental Biology*, *415*, 347–370.

Reif, W.-E. (1978). Wound healing in sharks. *Zoomorphologie*, *90*, 101–111.

Reif, W.-E. (1985). Functions of scales and photophores in mesopelagic luminescent sharks. *Acta Zoologica*, *66*, 111–118.

Rice, D. P., Aberg, T., Chan, Y., Tang, Z., Kettunen, P. J., Pakarinen, L., Maxson, R. E., & Thesleff, I. (2000). Integration of FGF and TWIST in calvarial bone and suture development. *Development*, *127*, 1845–1855.

Rosenquist, T. A., & Martin, G. R. (1996). Fibroblast growth factor signalling in the hair growth cycle: Expression of the fibroblast growth factor receptor and ligand genes in the murine hair follicle. *Developmental Dynamics*, *205*, 379–386.

Sansom, I. J., Smith, M. M., & Smith, M. P. (1996). Scales of the lodont and shark-like fishes from the Ordovician of Colorado. *Nature*, *379*, 628–630.

Schindelin, J., Arganda-Carreras, I., Frise, E., Kaynig, V., Longair, M., Pietzsch, T., Preibisch, S., Rueden, C., Saalfeld, S., Schmid, B., Tinevez, J. Y., White, D. J., Hartenstein, V., Eliceiri, K., Tomancak, P., & Cardona, A. (2012). Fiji: An open-source platform for biological-image analysis. *Nature Methods*, *9*, 676–682.

Seidensticker, M. J., & Behrens, J. (2000). Biochemical interactions in the Wnt pathway. *Biochimica et Biophysica Acta - Molecular Cell Research*, *1495*(2), 168–182.

Shyer, A. E., Rodrigues, A. R., Schroeder, G. G., Kassianidou, E., Kumar, S., & Harland, R. M. (2017). Emergent cellular self-organization and mechanosensation initiate follicle pattern in the avian skin. *Science*, *357*, 811–815.

Shyer, A. E., Tallinen, T., Nerurkar, N. L., Wei, Z., Gil, E. S., Kaplan, D. L., Tabin, C. J., & Mahadevan, L. (2013). Villification: How the gut gets its villi. *Science*, *342*, 212–218.

Sibert, E. C., & Rubin, L. D. (2021). An early Miocene extinction in pelagic sharks. *Science*, *372*, 1105–1107.

Sick, S., Reinker, S., Timmer, J., & Schlake, T. (2006). Wnt and DKK determine hair follicle spacing through a reaction-diffusion mechanism. *Science*, *314*, 1447–1450.

Sire, J.-Y., Donoghue, P. C. J., & Vickaryous, M. K. (2009). Origin and evolution of the integumentary skeleton in non-tetrapod vertebrates. *Journal of Anatomy*, *214*(4), 409–440.

Smith, M. M., & Coates, M. I. (1998). Evolutionary origins of the vertebrate dentition: Phylogenetic patterns and developmental evolution. *European Journal of Oral Sciences*, *106*, 482–500.

Smith, M. M., & Coates, M. I. (2000). Evolutionary origins of teeth and jaws: Developmental models and phylogenetic patterns. In M. F. Teaford, M. W. J. Ferguson, & M. M. Smith (Eds.), *Development, function and evolution of teeth*. Cambridge University Press.

Smith, M. M., & Coates, M. I. (2001). The evolution of vertebrate dentitions: Phylogenetic pattern and developmental models. In P. E. Ahlberg (Ed.), *Major events of early vertebrate evolution*. Taylor & Francis.

Smith, M. M., Fraser, G. J., Chaplin, N., Hobbs, C., & Graham, A. (2009). Reiterative pattern of sonic hedgehog expression in the catshark dentition reveals a phylogenetic template for jawed vertebrates. *Proceedings Biological Sciences*, *276*, 1225–1233.

St-Jacques, B., Dassule, H. R., Karavanova, I., Botchkarev, V. A., Li, J., Danielian, P. S., Mcmahon, J. A., Lewis, P. M., Paus, R., & Mcmahon, A. P. (1998). Sonic hedgehog signaling is essential for hair development. *Current Biology*, *8*, 1058–1069.

Thiery, A. P., Standing, A. S., Cooper, R. L., & Fraser, G. J. (2022). An epithelial signalling centre in sharks supports homology of tooth morphogenesis in vertebrates. *eLife*, *11*, e73173.

Vaahtokari, A., Åberg, T., Jernvall, J., Keränen, S., & Thesleff, I. (1996). The enamel knot as a signaling center in the developing mouse tooth. *Mechanisms of Development*, *54*, 39–43.

Vainio, S., Karavanova, I., Jowett, A., & Thesleff, I. (1993). Identification of BMP-4 as a signal mediating secondary induction between epithelial and mesenchymal tissues during early tooth development. *Cell*, *75*, 45–58.

Wen, L., Weaver, J. C., Thornycroft, P. J. M., & Lauder, G. V. (2015). Hydrodynamic function of biomimetic shark skin: Effect of denticle pattern and spacing. *Bioinspiration & Biomimetics*, *10*, 066010.

Wyffels, J., L. King, B., Vincent, J., Chen, C., Wu, C. H., & Polson, S. W. (2014). SkateBase, an elasmobranch genome project and collection of molecular resources for chondrichthyan fishes. *F1000Research*, *3*, 191.

Yu, T., & Klein, O. D. (2020). Molecular and cellular mechanisms of tooth development, homeostasis and repair. *Development*, *147*(2), dev184754.

SUPPORTING INFORMATION

Additional supporting information can be found online in the Supporting Information section at the end of this article.

How to cite this article: Cooper, R. L., Nicklin, E. F., Rasch, L. J., & Fraser, G. J. (2023). Teeth outside the mouth: The evolution and development of shark denticles. *Evolution & Development*, 25, 54–72. https://doi.org/10.1111/ede.12427